SYNERGY OF RADIOACTIVE ^{241}Am AND THE EFFECT OF HOLLOW CATHODE IN OPTIMIZING GAS-INSULATED SURGE ARRESTERS CHARACTERISTICS

by

Alija JUSIĆ [1*], ***Zijad BAJRAMOVIĆ*** [2], ***Irfan TURKOVIĆ*** [2], ***Adnan MUJEZINOVIĆ*** [2], ***and Predrag V. OSMOKROVIĆ*** [3]

[1]Power Electric Utility of Bosnia and Herzegovina, Sarajevo, Bosnia and Herzegovina
[2]Faculty of Electrical Engineering, University of Sarajevo, Sarajevo, Bosnia and Herzegovina
[3]Faculty of Electrical Engineering, University of Belgrade, Belgrade, Serbia

Scientific paper
http://doi.org/10.2298/NTRP1803260J

The paper discusses the possibility of improving the character of gas surge arresters. Examined were: the magnetic field effect, the effect of the hollow cathode, and the effect of the alpha radiation source ^{241}Am. Numerical and real experiments conducted are presented together with theoretical interpretations of the obtained results. Real experiments were carried out on a model of a gas surge arrester spatially constructed for experiments presented in this paper. The model was designed in such a way that it was possible to change all the relevant parameters of the gas surge arrester model. Experiments were conducted under well-controlled laboratory conditions. The tests were performed with d. c. and impulse voltage. The results obtained by experiments were processed by sophisticated statistical methods. The expressed measurement uncertainty of the experimental procedure showed a high statistical reliability of the obtained results. Based on the results of the research, the model of a gas surge arrester, in which the effect of the hollow cathode and the radioactive source ^{241}Am were combined, unambiguously proved to have the best characteristics.

Key words: gas surge arrester, radioactive isotope ^{241}Am, effect of the hollow cathode

INTRODUCTION

The gas surge arresters (GSA) are elements primarily utilized for overvoltage protection at the low voltage level. The main advantages of GSA are high power dissipation and a possibility to be used in the hybrid protection circuit. The main disadvantages of GSA are a relatively slow response, irreversible changes in characteristics over time and long-term deconditioning [1, 2].

The gas surge arrester consists of two identical metal electrodes in the ceramic or glass tube filled with noble gas at low pressure (in the German language known as a noble gas fuse). The electrodes are usually made of a material with a small value of the work function. The electric field in the interelectrode gap is homogeneous or pseudo homogenous. The working point of GSA is determined by product $p \times d$ (pressure × interelectrode distance) and should be stable during the time of exploitation. Commercially GSA with three electrodes is also available [3, 4].

* Author's e-mail: al.jusic@epbih.ba

Diverse papers have considered practical solutions and material selection with the aim of stabilizing working points of gas surge arresters thereby increasing the speed of their response [5, 6]. The recently published papers have considered and subsequently offered a solution of the problem of the GSA long-term deconditioning. Even though satisfactory results have been reported, the resulting solution is often in conflict with the demand for small or irreversible changes of gas insulation of GSA resulting in a life expectancy shortening. The GSA functioning is based on multiple breakdowns which cause changes on the electrodes surfaces and consequently changing the topography and other erosive properties. These breakdowns cause gas ionization and changes of the gas composition (particularly the composition property pertaining to electrode material evaporation). For that reason, GSA during some time (the dead or recovery time) is out of function.

The aim of this paper is to examine the possibility of achieving the positive synergistic effect on the characteristics of GSA using alpha radiation, the hollow cathode effect, and a magnetic field. The proposed method is predominantly experimental. Interpretation

of the obtained results is based on the interaction of nuclear radiation with material theory combined with electric discharges in gas dielectrics theory.

THEORETICAL BACKGROUND

Static gas breakdown

Self-sustained avalanche processes result in the electrical breakdown of any gas, which is dependent on the relative activity pertaining to the functioning of the generation-and-loss mechanism of an electron. Elementary processes in the gas are described as is required by mathematical modeling. Furthermore, avalanche coefficients are considered for these elementary processes. More specifically, the avalanche coefficients, which are the most frequently utilized, are the following ones:

- α-number of electronic ionization collisions per cm of distance in the direction of the electric field,
- η-number of electrons per cm of distance in the direction of the field attached to electrically negative atoms or molecules, and
- γ-number of electrons generated from secondary processes per each primary avalanche.

The constant value of certain gas or gas mixture is not obligatory for the avalanche coefficients. Moreover, this value varies with regard to pressure and electric field

$$\alpha(x) \quad pC_1 e^{-\frac{C_2}{E(x)/p}} \tag{1}$$

where C_1 and C_2 are experimentally determined constants. For helium, $C_1 = 2.1$ Pa^{-1}m^{-1} and $C_2 = 25.5$ V Pa^{-1}m^{-1}.

The value of γ coefficient is dependent upon many factors and, accordingly, has the scope from 10^{-4} to 10^{-9} [6].

The electrode geometry, as well as the variation of the avalanche coefficients, should be considered to calculate the lowest possible breakdown voltage value in a two-electrode system. The application of the rising voltage seems to be slow when compared with the time characteristics for the elementary processes in gas but leads to the lowest possible breakdown. Additionally, such a voltage is often referred to as the static voltage (d. c. voltage). It is the Townsend criterion that governs the static breakdown voltage in the case when the secondary processes on the electrodes (ionic discharge, photoemission, metastable discharge) control the secondary processes in gas (ionization by positive ions, photoionization, metastable ionization).

$$\gamma \int_o^d \exp\left[\int_0^x \alpha \mathrm{d}x\right] \alpha \mathrm{d}x \quad 1 \tag{2}$$

In the case when the secondary processes in gas dominate the secondary processes on electrodes, the static breakdown voltage is in the form of streamers that are determined by the criterion

$$\int_o^d \alpha \mathrm{d}x \quad 10.5 \tag{3}$$

Dynamic gas breakdown

Preliminary consideration of gas breakdown did not take into account the time of voltage load. For that reason, previous consideration is only valid when the time characteristic of load voltage is much longer than the time characteristic for elementary processes of electric discharge in gases. Such a breakdown, as mentioned, is called static voltage (d. c. voltage) gas breakdown. In the case when the characteristic time of voltage change is comparable with the characteristic time for elementary processes of electric discharge in gases, then it is an impulse gas breakdown. On the one hand, values of d. c. breakdown voltage (especially in a homogeneous field) are deterministic. On the other hand, values of impulse breakdown voltage are stochastic [7, 8]. In practice, gas insulation, influenced by impulse voltage, is characterized by the so-called volt-second characteristic. The volt-second characteristic is most often shown as an area in a volt-second plane in which are all values of impulse breakdown voltage with certain accuracy, regardless of the shape of the impulse itself. Since the experimental determination of impulse characteristic by time is irrational, it is usually used semi-empirical Area Law [9].

The derivation of the Area Law takes as its starting point the assumption that the plasma in the inter-electrode region extends at a rate $V(x, t)$ that exhibits the linear increase within the electric field [10]

$$V(x,t) \quad k[E(x,t) \quad E_S(x)] \tag{4}$$

where k is a factor depending on the voltage polarity, E_S – the electric field that corresponds to the d. c. breakdown voltage U_S. Furthermore, the electric field can be expressed as a product of a time-dependent and space dependent part

$$E(x,t) \quad U(t)g(x) \tag{5}$$

Assuming k is constant across the inter-electrode gap then

$$\frac{1}{k}\int_{t_1}^{t_1 \; t_a} \frac{\mathrm{d}x}{g(x)} \int_{t_1}^{t_1 \; t_a} [U(t) \quad U_S]\mathrm{d}t \quad P \quad \text{const.} \tag{6}$$

where t_1 refers to the moment at which the pulse of the load voltage attains the value of d. c. breakdown voltage, $x = x_k$ – the point within the region where the Townsend mechanism is converted into the streamer mechanism, and $t = t_1 + t_a$ – the instant that follows this change [11, 12]. Moreover, there must be a constant geometrical area P in the voltage-vs.-time coordinate system delimited by $U(t)$ and U_S to bring the occurrence of a breakdown, which follows from eq. (6).

If the 1 % and 99 % probability quantiles of impulse breakdown voltage and d. c. breakdown voltage are known, then the areas P_1 and P_{99} can be calculated from eq. 3. This is particularly possible through the determination of P_1 and P_{99} areas and displaying impulse characteristics of quantiles probability pertaining to

the impulse breakdown voltage the scope of which ranges between 1 % and 99 %. All values of the points (breakdown voltage, breakdown time) lie between these two impulse characteristics the probability of which is greater than 1 % and less than 99 %.

Electron in electromagnetic field

If a particle of mass m and charge q moves with velocity $\vec{V}$ in the direction normal to the lines of magnetic field induction $\vec{B}$ then Lorentz force $\vec{F}$ acts on the particle in the direction normal to $\vec{V}$ and $\vec{B}$. When the vectors $\vec{V}$ and $\vec{B}$ are orthogonal follows for Lorentz force $\vec{F}$, fig. 1

$$F_L \quad VBq \tag{7}$$

The radius r of the curvature of the particle path, the radius of its orbit, is determined by the balance between Lorentz force F_L and centrifugal force F which acts on the particle. From there it follows

$$r \quad \frac{mV}{qB} \tag{8}$$

The effect of the hollow cathode

The hollow cathode effect is very useful as an electronic generator. Within the cavity of the cathode, the electrons accelerate from one side of the cavity to the other and in the same time moving towards the anode. So, an electronic multiplication is performed under the condition that the diameter of the cavity is greater than the mean free path of an electron, fig. 2. This effect is also known as "pendulum effect" and it is estimated that it can produce the electronic current density of over 10 Acm^{-2}.

Calculation of d. c. breakdown voltage

To calculate d. c. breakdown voltage of the bi-electrode system insulated by gas under known pressure the following three parameters should be considered: (1) electric field in the inter-electrode gap;

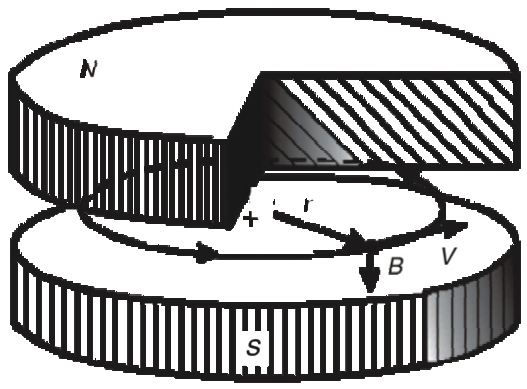

Figure 1. Illustration of the Lorentz force

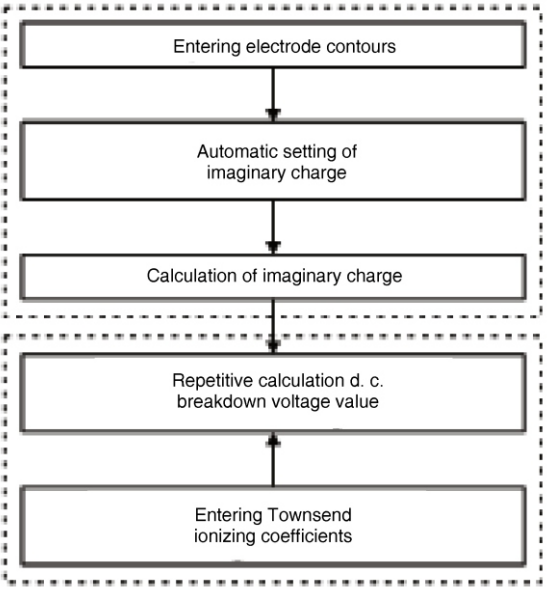

Figure 2. Flowchart for calculation of d.c. breakdown voltage value

(2) electrical breakdown mechanism, and (3) the Townsend ionization coefficient dependence *vs*. the ratio of electric field value and pressure.

The program specifically tailored and developed for the purposes of this paper calculated the electric field in the inter-electrode gap by means of the charge simulation method. Backed by the given electrode contours, a number of imaginary charges and number of control points the program was also able to determine on its own both the type and position of imaginary charge. Furthermore, the program was also capable of determining the position of control and contour points, the field lines, and equipotential lines as well as maximal electric field lines.

Provided that the working point of GSA is in the area where the Townsend breakdown mechanism is dominant, the breakdown voltage should be calculated by eq. 2. The Townsend ionizing coefficients were utilized to calculate d. c. breakdown voltage value, eq.1.

The definite calculation of d. c. breakdown voltage value was carried out by taking as a starting point an assumption of the linear increase of voltage (*vs*. a parameter t), while the fulfillment of condition (1) was checked for two points (so that the left side of the eq. 1 was less than zero at one point, while it was above zero in the other). We determined d. c. breakdown voltage value with predetermined error margin in an above-described way, and by utilizing the repetitive procedure. The program flow chart of d. c. breakdown voltage value calculation is given in fig. 2 [13].

Experiment and processing of experimental results

The experiments were carried out on the model of a gas-filled surge arrester (hereinafter referred to as model), fig. 4. The axially symmetrical model was de-

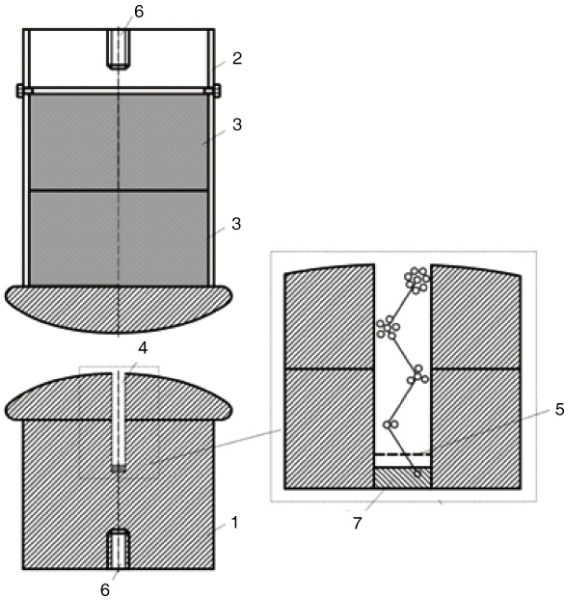

Figure 3. Electrode system and hollow cathode mechanism: *1 – hollow cathode type Rogovsky, 2 – anode type Rogovsky, 3 – Alnico magnets, 4 – the cavity, 5 – the mesh, 6 – the fine screw thread, 7 – ^{241}Am*

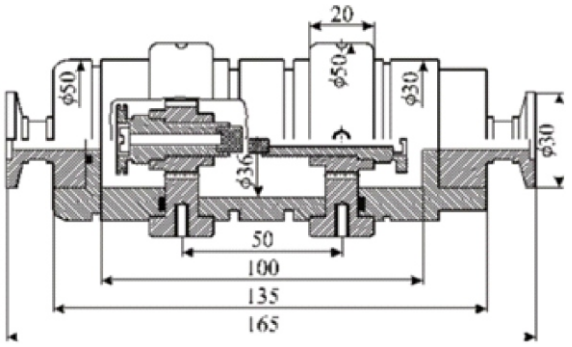

(a)

(b)

Figure 4. GFSA model: (a) model scheme and (b) model photo

signed so that was possible to change: 1 – electrodes; 2 – interelectrode distance; 3 – a type of working gas and 4 – the pressure of working gas. During the measurement, the model is placed in a permanent magnetic field directed along the axial axis.

The used electrodes were made of brass with a form of Rogovsky. For every interelectrode distance, another pair of electrodes was made in accordance with the equipotential calculation of the electric field in the interelectric space (the edge of the electrode type Rogovsky follows the equipotential line). The method of the electric charge simulation was used for calculating the electric field [14]. A cavity with the radius of 0.1 mm and a depth of 1 mm was formed along the coaxial axis in the electrode which was used as a cathode. At the bottom of this cavity was ^{241}Am (α emitter, 5.6 MeV, 432 years halftime) protected by a mesh. On the underside of the anode there was a possibility to insert one or two cylindrical magnets whose ratio of height and radius was 1 and remnant induction was 0.25 T. The magnetic field along the axial axis was 0.085 T and 0.11 T, see fig. 3. Before each installation, the electrodes are polished to high gloss.

The interelectrode distance was set in the following way: 1 – the electrodes are brought to distance 0 (what is determined by measuring electrical resistance between the electrodes); 2 – adjustment of the interelectrode distance by the rotate shifting of the electrode mobile holder and by digital micrometer and 3 – strengthening of the electrode mobile holder. The interelectrode distances during the measurement were 0.2 mm, 0.5 mm, and 1 mm. During the measurement, the pressure varied from 5000 Pa to 50000 Pa, steps 500 Pa.

Choice of working gas type and adjusting pressure values was made using a gas circuit shown in fig. 5. The pressure adjustment was carried out during the installation of the chamber in the gas circuit in the following way: 1 – vacuuming the chamber and the gas circuit to pressure 1 mPa; 2 – filling with working gas up the pressure of 105 Pa; 3 – repeating 3 times the steps 1 and 2 with final vacuuming; 4 – adjusting the desired pressure value (with needle valve) reduced to 0 °C and 5 – turning the chamber on generator. The high purity Helium was used as a working gas.

The d. c. generator had a flow rate 8 Vs^{-1}. The value of the breakdown voltage was measured by ohm voltage divider and memory voltmeter. The impulse generator was adjusted on a standard atmospheric volt-

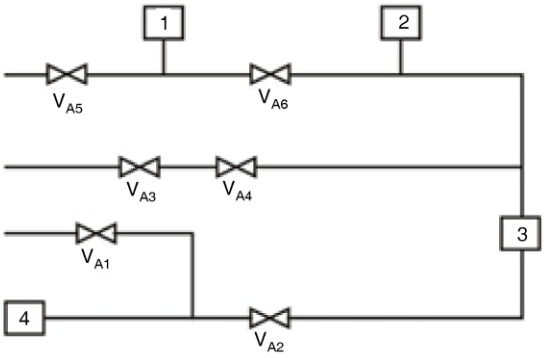

Figure 5. Gas circuit; 1 – absolute instrument, 2 – relative instrument, 3 – chamber, 4 – vacuum pump, V_{A1}, V_{A2}, V_{A3}, V_{A5}, V_{A6} are two-position valves, V_{A4} is a dosing valve (needle valve)

age impulse with shape 1.2/5 μs of the amplitude. The impulse breakdown voltage was measured with compensated capacitor divider and with the oscilloscope of 500 MHz. The memory voltmeter and the oscilloscope were placed during the measurement in the protective cabin with protection greater than 100 dB. The protective cabin had its own power supply and was galvanically separated from the measuring system.

For one value of d. c. breakdown voltage, 20 values of the d. c. breakdown voltage were measured. For one value of the impulse breakdown voltage, 100 values of the impulse breakdown voltage were measured. Such selection of the statistical samples size provided reliable statistical conclusions according to *t*-test. A break of 1 minute was made between the two successive breakdowns. Prior to each measurement series, the electrode system was conditioned with 50 successive breakdowns of d. c. voltage. For determining impulse characteristic, 5000 impulse breakdown voltages and 20 d. c. breakdown voltages were measured for the same value of pd variable. The obtained statistical samples of the random variables "d. c. breakdown voltage" and "impulse breakdown voltage" were processed as follows: 1 – purification of the statistical sample from suspected measurement results by using the modified Chauvenet's criterion; 2 – checking the belonging of all random variables "d. c. breakdown voltage" to the same statistical sample by using the U test; 3 – testing the statistical samples for affiliation on Normal, Weibull and Double exponential distribution; 4 – determination of the central moments from the obtained statistical samples.

Based on the obtained experimental results, d. c. and impulse Paschen curves points were determined. In addition to experimental points of d. c. Paschen curves, theoretical curves are drawn, obtained on the basis of the Townsend criterion, eq. 2. Beside d. c. and impulse Paschen curves, the impulse characteristics are drawn based on the Area Law. In doing so, all parameters of the experiment were changed: 1 – cathode with and without cavity; 2 – hollow cathode with and without a radioactive sample; 3 – the value of magnetic induction along the axial axis of the interelectrode distance (0 T, 0.085 T, and 0.11 T); 4 – the interelectrode distance.

The measurement uncertainty Type A is determined by methods of mathematical statistics. The measurement uncertainty Type B is determined by Monte Carlo and analytical methods. In the measurement uncertainty Type B are included the measurement uncertainty Type B of all used instruments (given by producers). The combined measurement uncertainty is determined by a method from the references [15-17] and was less than 7 %.

RESULTS AND DISCUSSIONS

As shown in fig. 6 the experimentally obtained values of d. c. breakdown voltage depending on the pressure of the gas He. The interelectrode distance was

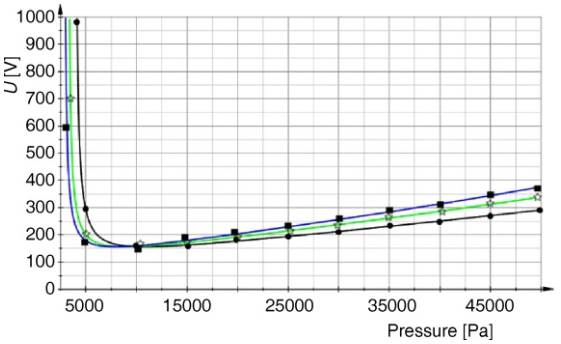

Figure 6. The experimentally obtained values of d. c. breakdown voltages versus pressure fitted by Paschen curve with an interelectrode gap as the parameter:
• *– the electrodes type Rogovsky;* ⋆ *– the electrodes type Rogovsky with the magnetic field 0.085T in the interelectrode gap;* ■ *– the electrodes type Rogovsky with the magnetic field 0.11T in the interelectrode gap*

0.5 mm. The shown experimental results refer to the next cases: 1 – anode type Rogovsky, cathode type Rogovsky, without the magnetic field; 2 – anode type Rogovsky, cathode type Rogovsky, with the magnetic field 0.085 T; 3 – anode type Rogovsky, cathode type Rogovsky, with the magnetic field 0.11 T; 4 – anode type Rogovsky, cathode type Rogovsky, with cavity, without the magnetic field and 5 – cathode type Rogovsky, with ^{241}Am as the radiation source in the cavity. In addition to the experimentally obtained points, in fig. 7 are also shown the following curves: 1 – theoretical dependence of d. c. breakdown voltage values from the pressure for the interelectrode distance 0.5 mm (according to Paschen criterion); 2 – fitted curves dependency of the breakdown voltage values from the pressure, for the interelectrode distance as a parameter (with the magnetic field 0.085 T); 3 – fitted curves dependency of the breakdown voltage values from the pressure, for the interelectrode distance as a parameter (with the magnetic field 0.11 T).

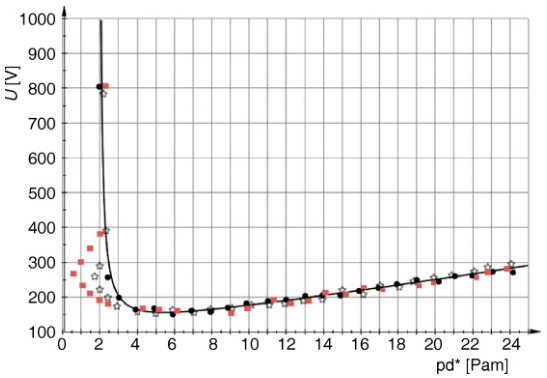

Figure 7. The experimentally obtained values of d. c. breakdown voltages *vs.* pd product and theoretically determined Paschen curve;
■ *– the electrodes type Rogovsky with the magnetic field 0.11 T in the interelectrode gap;* ⋆ *– the electrodes type Rogovsky with the magnetic field 0.085 T in the interelectrode gap;* • *– the electrodes type Rogovsky with ^{241}Am as the radiation source in the cavity*
*pd – product of pressure and interelectrode distance

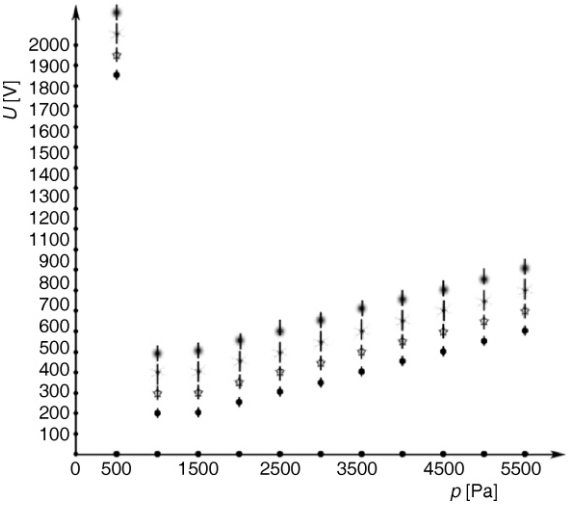

Figure 8. Values of the impulse breakdown voltages with error bars: • *anode type Rogovsky, cathode type Rogovsky, with ^{241}Am as the radiation source in the cavity;* ⊛ *anode type Rogovsky, cathode type Rogovsky, with the magnetic field;* ✲ *anode type Rogovsky, cathode type Rogovsky, with cavity;* ✲ *anode type Rogovsky, cathode type Rogovsky, without the magnetic field*

As shown in fig. 7 the experimentally obtained values of Paschen curve for He refer to the next cases: 1 – anode type Rogovsky, cathode type Rogovsky, without the magnetic field and 2 – anode type Rogovsky, with the magnetic field 0.085 T, cathode type Rogovsky, with ^{241}Am as the radiation source in the cavity. In addition to the experimentally obtained points, in fig. 7. the corresponding Paschen curve obtained according to Townsend criterion is also shown.

As shown in fig. 8 the experimentally obtained values of the impulse breakdown voltage depend on the pressure of the gas He. The interelectrode distance was 0.5 mm. The shown experimental results refer to the next cases: 1 – anode type Rogovsky, cathode type Rogovsky, without the magnetic field; 2 – anode type Rogovsky, cathode type Rogovsky, with the magnetic field; 3 – anode type Rogovsky, cathode type Rogovsky, with cavity, and 4 – anode type Rogovsky, cathode type Rogovsky, with ^{241}Am as the radiation source in the cavity.

As shown in fig. 9 1 % and 99 % impulse characteristics obtained by the impulses 1.2/50 μs and by the Area Law refer to the next cases: 1 – anode type Rogovsky, cathode type Rogovsky and 2 – anode type Rogovsky, cathode type Rogovsky, with the magnetic field 0.085 T.

As shown in fig. 10 1 % and 99 % impulse characteristics obtained by the impulses 1.2/50 μs and by the Area Law refer to the next cases: 1 – anode type Rogovsky, cathode type Rogovsky, with cavity and 2 – anode type Rogovsky, cathode type Rogovsky, with ^{241}Am as the radiation source in the cavity.

The results depicted in fig. 6 show that: 1 – the experimentally obtained results for the electrode configuration anode type Rogovsky – cathode type Rogovsky

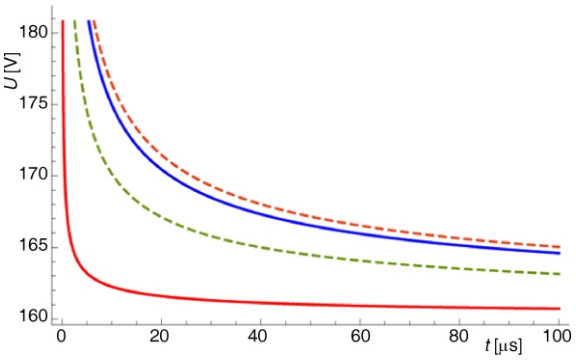

Figure 9. 1 % and 99 % impulse characteristics for the electrode configuration: — *anode type Rogovsky, cathode type Rogovsky without the magnetic field (diagrams 1 and 2 respectively);* **— — —** *anode type Rogovsky, cathode type Rogovsky, with the magnetic field 0.085 T(diagrams 3 and 4 respectively)*

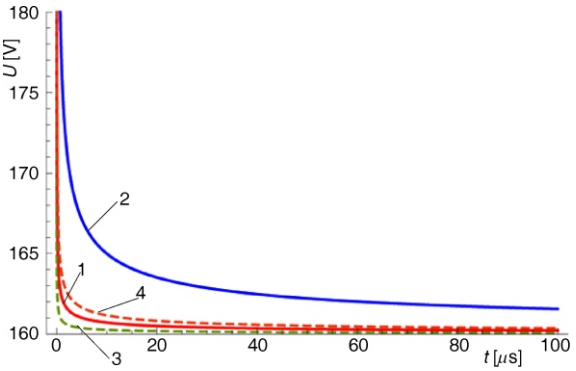

Figure 10. 1% and 99% impulse characteristics for the electrode configuration: - - *anode type Rogovsky, cathode type Rogovsky), with a cavity(diagrams 1 and 2 respectively;* **- - -** *anode type Rogovsky, cathode type Rogovsky, with ^{241}Am as the radiation source in the cavity(diagrams 3 and 4 respectively)*

agree well with a theoretically calculated curve in the points on the right side of the minimum. In the points on the left side next to the minimum, comes to standard deviation between the theoretically calculated values and experimentally obtained values. The difference left to the minimum can be explained by the Anomalous Paschen effect (especially characteristic for electrodes type Rogovsky [17]); 2 – the experimentally obtained results for the electrode configuration anode type Rogovsky – cathode type Rogovsky with the magnetic field 0.085 T in the interelectrode gap, show higher values than the results obtained without magnetic field. The difference between these two result groups is about 10 % right to the minimum. The difference left to the minimum is significantly lower and is within the statistical error. Such a result can be explained by the effective increase of the interelectrode distance due to the magnetic field. This conclusion is confirmed by the fact that with fitting the results a very good agreement was obtained right to the minimum for $d = 0.61$ mm (d is the interelectrode distance). In the points on the right side

of the minimum the magnetic field brings to the increase of the Anomalous Paschen effect; 3 – the experimentally obtained results for the electrode configuration anode type Rogovsky – cathode type Rogovsky with the magnetic field 0.11 T in the interelectrode gap, show the same behavior as when the magnetic field is 0.085 T but only strongly expressed; 4 – the experimentally obtained results for the electrode configuration anode type Rogovsky – cathode type Rogovsky with the cavity and without cavity have good agreement. The only difference is when the cathode is with the cavity; then it comes to decreasing of the standard deviation for the statistical samples of the random variables d. c. breakdown voltage (about 50 %); 5 – the experimentally obtained results for the electrode configuration anode type Rogovsky – cathode type Rogovsky with and without ^{241}Am as the radiation source in the cavity have good agreement. The basic difference is that the standard deviation for the statistical sample of the random variable d. c. breakdown voltage is zero when ^{241}Am is in the cathode cavity. This result is very important for the use of the gas surge arresters.

As can be seen in fig. 7 the Anomalous Paschen effect occurs in the points left from the Paschen minimum for all three configurations of the electrodes. The Anomalous Paschen effect is most expressed for the electrode configuration anode type Rogovsky, cathode type Rogovsky with the magnetic field. The Anomalous Paschen effect is least expressed for the electrode configuration anode type Rogovsky, cathode type Rogovsky with ^{241}Am. This result is explained as follows: 1 – in the case when the magnetic field is present in the interelectrode gap, the breakdown may occur along a number of field lines of various lengths of electron paths and 2 – in the case when radioactive source ^{241}Am is present, concentration of free electrons, potentially initial, is significantly higher in the center of the interelectrode gap than in the edge areas of electrodes so all breakdowns take place in central area of the interelectrode gap (along the shortest line of the electric field equal to interelectrode distance).

The results depicted in fig. 8 show that mean values and standard deviation for the statistical sample of the random variable d. c. breakdown voltage have higher values with the magnetic field. The increase of the standard deviation is higher than the increase of the mean value. Lower magnetic field values correspond to lower increase of standard deviation and mean value (for $B = 0.085$ T, $\Delta\overline{U}$ 10 %, $\Delta\sigma$ 14 %; for $B = 0.11$ T, $\Delta\overline{U}$ 17 %, $\Delta\sigma$ 21 %).

The results depicted in fig. 9 show that the magnetic field in the interelectrode distance raises the voltage level of the impulse characteristics. Also, the magnetic field expands the area between 1 % and 99 % of the impulse characteristics. These are undesirable effects for the protective function of the surge arrester.

The results depicted in fig. 10 show that the electrode configuration anode type Rogovsky – cathode type Rogovsky with cavity lowers voltage level of the impulse characteristics and narrows the area between 1 % and 99 % of the impulse characteristics regarding the configuration without a cavity. Based on the latter, it can be concluded that the effect of the hollow cathode improves characteristic of the gas surge arresters. However, the same figure shows that when ^{241}Am is in the cathode cavity, the characteristics of the gas surge arresters are drastically improved.

CONCLUSIONS

The discussed possibilities of improving the protection characteristics of gas surge arresters gave two results. Both results can be considered significant. It was found that the gas surge arrester in the magnetic field loses its nominal characteristics *i. e.* there is an increase in the conductivity characteristics. Such a change threatens the protected components because the parameters were changed according to which the calculation of coordinating isolation at the low voltage level was performed. This result is important to consider when there is a possibility that the gas surge arrester could be in the magnetic field during operation. Another, more significant, is the result that ^{241}Am as the radiation source in the cathode cavity substantially improves the protective characteristics of the gas surge arresters. This effect is due to the synergy of the hollow cathode effect and the effect of ionizing radiation. The gas surge arresters, designed to consider this effect, made the results of coordinating isolation much more reliable. This solution also has a bad side because it involves the introduction of radioactivity into the environment. This disadvantage, however, is easily resolved by legislation. It is important to emphasize that the effects tested on gas surge arresters for low voltages according to Model law can be used for gas surge arresters on high voltages.

AUTHORS' CONTRIBUTIONS

The numerical simulations were prepared, carried out and post-processed by A. Jusić. A. Jusić, Z. Bajramović, I. Turković, A. Mujezinović, and P. V. Osmokrović have done theoretical research and parameter fitting. P. V. Osmokrović has designed the measuring circuit. The figures and tables were prepared by A. Jusić. The manuscript was prepared and revised jointly by all the authors.

REFERENCES

[1] Hasse, P., Overvoltage Protection of Low Voltage Systems; IEE Power & Energy Series 33; The Institution of Engineering and Technology: London, 2000
[2] Standler, R. B., Protection of Electronic Circuits from Overvoltages; Dover Books on Electrical Engineering, Mineola, New York, USA, 2002
[3] Pejović, M. M., *et al*., Experimental Investigation of Breakdown Voltage and Electrical Breakdown Time Delay of Commercial Gas Discharge Tubes, *Japanese Journal of Applied Physics, 50* (2011), 8R

[4] Gopikishan, S., *et al*., Paschen Curve Approach to Investigate Electron Density and Deposition Rate of Cu in Magnetron Sputtering System, *Radiation Effects and Defects in Solids, 171* (2016), 11-12, pp. 999-1005
[5] Stanković, K., *et al*., Reliability of Semiconductor and Gas-Filled Diodes for Over-Voltage Protection Exposed to Ionizing Radiation, *Nucl Technol Radiat, 24* (2009), 2, pp. 132-137
[6] Lončar, B., *et al*., Radioactive Reliability of Gas Filled Surge Arresters, *IEEE Transactions on Nuclear Science, 50* (2003), 5 III, pp. 1725-1731
[7] Geibig, K. F., *et al*., Application of Phase-Bonded Materials in Spark Gaps, (*in German), 14* (1983), 6, pp. 197-201
[8] Veverka, A., Kvasnicka, V., Die Weibullverteilung und Die Konventionelle Abhangigkeit Der Durchschlagwahrscheinlichkeit (Tschech.), Elektrotechn, *Obzor, 67* (1978), 3, pp. 135-137
[9] Stanković, K., *et al*., Long-Term Deconditioning of Gas-Filled Surge Arresters, *Radiation Effects and Defects in Solids, 171* (2016), 7-8, pp. 678-691
[10] Paus, L., Cortina, R., Switching and Lightning Impulse Discharge Characteristics of Air Gaps and Station Insulators, *IEEE Trans., PAS 87* (1968), 4, pp. 947-957
[11] Osmokrović, P., Electrical Breakdown of SF6 at Small Values of the Product pd, *IEEE Transactions on Power Delivery, 4* (1989), 4
[12] Hauschild, W., Mosch, W., Statistical Techniques for High-Voltage Engineering, 1992 Peter Peregrinus Ltd., London
[13] Luka, P., *et al*., Influence of the Percentage Share of Electronegative Gas in the Mixture with Noble Gas on the Free-Electron Gas Spectrum and Recovery Time, *IEEE Transactions on Dielectrics and Electrical Insulation, 24* (2017), 5, pp. 2765-2774
[14] Osmokrović, P., *et al*., Reliability of Three-Electrode Spark Gaps, *Plasma Devices and Operations, 16* (2008), 4, pp. 235-245
[15] Kovačević, A. M., *et al*., The Combined Method for Uncertainty Evaluation in Electromagnetic Radiation Measurement, *Nucl Technol Radiat, 29* (2014), 4, pp. 279-284
[16] Kovačević, A. M., *et al*., Uncertainty Evaluation of the Conducted Emission Measurements, *Nucl Technol Radiat, 28* (2013), 2, pp. 182-190, pp. 221-227
[17] Geibig, K. F., *et al*., Use of Fiber-Reinforced Composite Materials in Sparking Gaps, (in German) *Zeitschrift Fuer Werkstoff technik, 14* (1983), 6, pp. 197-201

Received on May 15, 2018
Accepted on May 21, 2018

**Алија ЈУСИЋ, Зијад БАЈРАМОВИЋ, Ирфан ТУРКОВИЋ,
Аднан МУЈЕЗИНОВИЋ, Предраг В. ОСМОКРОВИЋ**

СИНЕРГИЈА РАДИОАКТИВНОГ ^{241}Am И ЕФЕКТА ШУПЉЕ КАТОДЕ НА ОПТИМИЗАЦИЈУ КАРАКТЕРИСТИКА ГАСНИХ ОДВОДНИКА ПРЕНАПОНА

У раду се разматра могућност унапређење карактеристика гасних одводника пренапона. Испитивани су: дејство магнетног поља, дејство ефекта шупље катоде и дејство извора алфа зрачења ^{241}Am. Обављани су нумерички експерименти, реални експерименти и теоретска тумачења добијених резултата. Реални експерименти су рађени на моделу гасног одводника пренапона. Модел је тако конципиран да је било могуће мењати све релевантне параметре. Експерименти су рађени под добро контролисаним лабораторијским условима. Испитивања су обављана јеносмерним и импулсним напоном. Добијени резултати су обрађивани софистицираним статистичким методама. Изражена мерна несигурност експерименталног поступка је показала високу статистичку поузданост добијених резултата. На основу резултата истраживања недвосмислено је доказано да најбоље карактеристике има модел гасног одводника пренапона у коме се комбинује ефекат шупље катоде и радиоактивни извор ^{241}Am.

Кључне речи: гасни одводник пренапона, радиоактивни изотоп ^{241}Am, ефекат шупље катоде